Wave dispersion near cyclotron resonance in pulsar plasmas

D. B. Melrose* and Q. Luo†
School of Physics, The University of Sydney, Sydney, NSW 2006, Australia
(Received 4 March 2004; published 23 July 2004)

In a standard pulsar model, the radio emission is produced in the relativistic, strongly magnetized electron-positron plasma in the polar-cap region of the magnetosphere. Waves are generated well below the cyclotron frequency and must propagate through the cyclotron resonance region where they are affected by the resonance. Wave dispersion near the cyclotron resonance is discussed in the formalism of the weak anisotropy approximation in which the relevant waves are treated as transverse. Analytical approximations for the two orthogonal modes are derived, in the rest frame of the plasma, for nearly parallel, nearly antiparallel and nearly perpendicular propagation with respect to the magnetic field direction. It is shown that due to the relativistic distribution the wave dispersion varies smoothly across the resonance with initially elliptical polarization evolving to linear and then elliptical polarization with opposite handedness. The relevance of such a change in handedness to the interpretation of circular polarization is discussed.

DOI: 10.1103/PhysRevE.70.016404 PACS number(s): 52.27.Ny, 52.27.Ep, 52.35.Ra, 52.35.Mw

I. INTRODUCTION

The pulsar plasma in which pulsar radio emission is generated, and through which it propagates along an escape path, is a strongly magnetized, non-charge-neutral, electron-positron pair plasma that is streaming highly relativistically along the magnetic field lines with highly relativistic random particle motions in its rest frame [1–4]. Pulsar radio emission is generated at frequencies well below the relativistic cyclotron frequency Ω_e/γ of the particles with typical Lorentz factors γ [5,6]. Along any prospective escape path, the waves must pass through the cyclotron resonance, where they can be affected by cyclotron absorption [7–10]. There is strong evidence that, in at least some pulsars, the radiation emerges in two orthogonally polarized modes [11,12], which can be significantly elliptically polarized [13,14]. The polarization of the orthogonal modes (OM's) must be characteristic of some polarization limiting region (PLR), beyond which generalized Faraday rotation [15,16] due to the pair plasma is ineffective in causing further changes to the polarization of the escaping radiation. The location of the PLR is poorly determined, but on general grounds one expects it to be associated with a region where the polarizations of the OM's are changing rapidly with distance along the ray path [17]. Dispersion associated with the cyclotron resonance can cause the polarization of the OM's to change rapidly as a function of frequency ω and angle θ of propagation. In order to discuss the propagation of radiation through the region of the cyclotron resonance, one needs a model for the dependence of the polarizations of the OM's of ω, θ, and various plasma parameters. Although a formal theory for dispersion in a pulsar plasma is available [18–24], this does not lead directly to useful analytical expressions for the dispersion relations or the polarization vectors.

In this paper we use an approximate method, referred to as the weak anisotropy approximation [25,26], to derive relatively simple analytical results for the dispersion relations and polarization vectors for frequencies that span the cyclotron resonance in a pulsar plasma. The basic idea in the weak anisotropy approximation is to assume that, to a first approximation, the medium is isotropic, so that the natural wave modes have two degenerate states of transverse polarizations. The anisotropy is included in the wave equation for transverse waves as a perturbation that breaks this degeneracy. The full wave equation is projected onto the transverse plane and any longitudinal part of the polarization is ignored. The solution of the resulting two-dimensional wave equation leads to relatively simple analytical results. A weakness of the method is that its region of validity is not obvious and the validity of the approximate analytic results needs to be checked against numerical solutions of the exact wave equation. In particular, the method breaks down near plasma resonances, where the waves become significantly longitudinal, raising the question as to whether it breaks down near the cyclotron resonance. In a highly relativistic plasma, the spread in Lorentz factors implies that the cyclotron resonance occurs over a broad frequency range, and this effectively smears out the resonance. The weak anisotropy approximation applies only if this smearing effect ensures that the refractive indices remain sufficiently close to unity throughout the cyclotron resonance region.

In Sec. II, a covariant form of the linear response tensor is written in terms of relativistic plasma dispersion functions (RPDF's). The general formalism of the weak anisotropy approximation is discussed in Sec. III, and an approximate expression for the dispersion relation at small propagation angles is derived in Sec. IV. The result of numerical calculation is discussed in Sec. V, and possible application to the interpretation of circular polarization in the pulsar radio emission is discussed in Sec. VI.

II. RESPONSE TENSOR

It is convenient to define a linear response four-tensor $t^{\mu\nu}(k)$ by $\mu_0 J^\mu(k) = t^{\mu\nu}(k) A_\nu(k)$, where $J(k)$, $A(k)$ are the Fou-

*Electronic address: melrose@physics.usyd.edu.au
†Electronic address: luo@physics.usyd.edu.au

rier transforms of the induced four-current and the four-potential, respectively. One form of the response tensor for a strictly one-dimensional pair plasma is [23]

$$t^{\mu\nu}(k) = -\omega_p^2 \int dp \frac{F(p)}{\gamma}\Bigg\{ -\frac{k_D^\mu k_D^\nu c^2}{(ku)^2} + \frac{1}{(ku)^2-\Omega_e^2}[(ku)^2 g_\perp^{\mu\nu} - ku(k_\perp^\mu u^\nu + u^\mu k_\perp^\nu) - k_\perp^2 u^\mu u^\nu + i\eta\Omega_e(kuf^{\mu\nu} + k_G^\mu u^\nu - u^\mu k_G^\nu)]\Bigg\}, \quad (1)$$

where the momentum $p^\mu = mu^\mu = \gamma mc(1,0,0,\beta)$ is strictly along the magnetic field, so that one has $ku = \gamma(\omega - k_\parallel \beta c)$, $\gamma = (1-\beta^2)^{-1/2}$. The one-dimensional distribution is normalized such that $\int dp\, F(p)$ is the number density, denoted $n^\pm$ for electrons and positrons, respectively, and the plasma frequency is defined by $\omega_p^2 = e^2(n^+ + n^-)/\varepsilon_0 m$. The difference between the electrons and positrons appears in $\eta = (n^+ - n^-)/(n^+ + n^-)$. The Maxwell tensor for the magnetostatic field is written $F^{\mu\nu} = Bf^{\mu\nu}$, $B = (F^{\mu\nu}F_{\mu\nu}/2)^{1/2}$, and then $g_\perp^{\mu\nu} = -f_\alpha^\mu f^{\alpha\nu}$, $g_\parallel^{\mu\nu} = g^{\mu\nu} - g_\perp^{\mu\nu}$ are the metric tensors in the 12-plane orthogonal to both the magnetic field, chosen to be along the 3-axis, and the time (0-) axis, and in the 03-plane defined by these two axes, respectively. These two tensors are combined with the wave four-vector, $k^\mu = (\omega/c, k_\perp, 0, k_\parallel)$ to construct four orthogonal four-vectors, three of which appear in Eq. (1):

$$k_\parallel^\mu = (\omega/c, 0, 0, k_\parallel), \quad k_\perp^\mu = (0, k_\perp, 0, 0),$$

$$k_G^\mu = (0, 0, k_\perp, 0), \quad k_D^\mu = (k_\parallel, 0, 0, \omega/c). \quad (2)$$

The integrals in Eq. (1) may be evaluated in terms of three RPDFs [23], by first writing the denominators as products of factors linear in β. It is convenient to write the zero of ku and the two zeros of $(ku)^2 - \Omega_e^2$ as $\beta = z$ and $\beta = z_\pm$, respectively, with

$$z = \frac{\omega}{k_\parallel c}, \quad y = \frac{\Omega_e}{k_\parallel c},$$

$$z_\pm = \frac{z \pm y(1+y^2-z^2)^{1/2}}{1+y^2}. \quad (3)$$

The RPDFs that appear may then be defined by

$$W(z) = \left\langle \frac{1}{\gamma^3(\beta - z)^2} \right\rangle,$$

$$R(z) = \left\langle \frac{1}{\gamma(\beta - z)} \right\rangle,$$

$$S(z) = \left\langle \frac{1}{\gamma^2(\beta - z)} \right\rangle, \quad (4)$$

where angular brackets denote the average over the distribution function. The specific functions that arise are $W(z)$, $R(z_\pm)$, and $S(z_\pm)$, with $W(z)$ characterizing the dispersion associated with the Landau resonance, and $R(z_\pm)$, $S(z_\pm)$ characterizing the dispersion associated with the normal and anomalous Doppler resonances, involving transitions between the ground state and the first Landau level.

III. THE WEAK ANISOTROPY APPROXIMATION

A. General formalism

The wave equation in the weak anisotropy approximation reduces to a two-dimensional equation for the four-potential in the radiation gauge, with the timelike and longitudinal components assumed to be zero. This wave equation is

$$[k^2 \delta_\nu^\mu + t_\nu^\mu(k)]A^\nu(k) = 0, \quad (5)$$

where μ, ν run over only the two transverse components, labeled 1, 2 here. In the coordinate system used in Eq. (2) we choose

$$e_1^\mu = (0, \cos\theta, 0, -\sin\theta), \quad e_2^\mu = (0,0,1,0), \quad (6)$$

with $\sin\theta = k_\perp/|\mathbf{k}|$, $\cos\theta = k_\parallel/|\mathbf{k}|$.

Writing Eq. (5) as a matrix equation and setting the determinant of the coefficients to zero gives the dispersion equation. Solving for the invariant $k^2 = \omega^2/c^2 - k_\perp^2 - k_\parallel^2$ gives

$$k^2 = k_\pm^2 = -\frac{1}{2}(t_1^1 + t_2^2) \pm \frac{1}{2}[(t_1^1 + t_2^2)^2 + 4t_2^1 t_1^2]^{1/2}, \quad (7)$$

with $t_2^1 = -t_1^2$ pure imaginary in a magnetoactive plasma. In terms of the refractive indices, $n_\pm^2$, Eq. (7) corresponds to $k_\pm^2 = (1 - n_\pm^2)\omega^2/c^2$. The eigenfunctions of Eq. (5) then give the polarization vectors in the radiation gauge. These are

$$e_\pm^\mu = \frac{T_\pm e_1^\mu + i e_2^\mu}{(T_\pm^2 + 1)^{1/2}}. \quad (8)$$

The polarization vector (8) corresponds to orthogonal elliptical polarizations with axial ratios

$$T_\pm = \frac{t_1^1 - t_2^2 \pm [(t_1^1 - t_2^2)^2 + 4t_2^1 t_1^2]^{1/2}}{2it_2^1}, \quad (9)$$

with the orthogonality of the two modes corresponding to $T_+ T_- = -1$.

The transverse components of the response tensor (1) evaluated in terms of the relativistic dispersion functions (4) give

$$t_1^1 = -\frac{\omega_p^2}{c^2}\Bigg\{ z^2 W(z)\sin^2\theta + \frac{1}{(1+y^2)\cos^2\theta}\Bigg[\left\langle \frac{1}{\gamma} \right\rangle + \frac{1}{z_+ - z_-}\sum_{\alpha = \pm} \alpha(z\cos^2\theta - z_\alpha)^2 R(z_\alpha)\Bigg]\Bigg\},$$

$$t_2^2 = -\frac{\omega_p^2}{c^2}\frac{1}{1+y^2}\Bigg[\left\langle \frac{1}{\gamma} \right\rangle + \frac{1}{z_+ - z_-}\sum_{\alpha = \pm} \alpha(z - z_\alpha)^2 R(z_\alpha)\Bigg],$$

$$t_2^1 = -i\eta\frac{\omega_p^2}{c^2}\frac{y}{(1+y^2)\cos\theta}\frac{1}{z_+ - z_-}\sum_{\alpha=\pm}\alpha(z\cos^2\theta - z_\alpha)S(z_\alpha), \tag{10}$$

with z, y, $z_\pm$ defined by Eq. (3). Note that the mixed spatial components t_j^i in the four-tensor formalism are equivalent to the corresponding components of the conventional three-tensor response such as in Refs. [23,24].

B. Conditions for the weak anisotropy approximation

The weak-anisotropy limit is valid only if the components of $t^{\mu\nu}$ are small compared with ω^2/c^2. Specifically, assuming $k^2=0$ to a zeroth approximation, the components (10) with $z=\sec\theta$, $y=(\Omega_e/\omega)\sec\theta$ must be small compared with ω^2/c^2. In a highly relativistic plasma $\langle\gamma\rangle \gg 1$, the maximum value of $W(z)$ is slightly greater than its value at $z=1$, specifically $W(1)\approx 2\langle\gamma\rangle$. The term involving $W(z)$ is compatible with the weak anisotropy approximation for $\omega^2 \gg \omega_p^2\langle\gamma\rangle$. This requires that the frequency be well above the frequency at which parallel longitudinal waves have a resonance, which becomes the maximum frequency for Alfvén waves for slightly oblique propagation [6].

The maximum values of the other two RPDFs, which determine the effects of the cyclotron resonance, are $|R(z_\pm)| \sim \langle\gamma\rangle$ and $|S(z_\pm)| \sim 1$, as shown below for a specific distribution. It follows that the components (10) are small, in the required sense, provided that the condition $\Omega_e^2 \gg \omega_p^2\langle\gamma\rangle$ is satisfied. This condition may be expressed in terms of the Alfvén speed, v_A, whose conventional definition corresponds to $v_A^2/c^2 = \Omega_e^2/\omega_p^2\langle\gamma\rangle$. The inclusion of the displacement current implies that the characteristic phase speed of magnetoacoustic and Alfvén waves is $v_A/(1+v_A^2/c^2)^{1/2}$. The condition $v_A^2/c^2 = \Omega_e^2/\omega_p^2\langle\gamma\rangle \gg 1$ ensures that the phase speeds of the waves is close to the speed of light through the region of the cyclotron resonance.

IV. APPROXIMATE RPDFs

It is desirable to have analytic approximations to the RPDFs $W(z)$, $R(z_\pm)$, $S(z_\pm)$, specifically approximations that apply near the cyclotron resonance in the relativistic limit. The RPDFs have been evaluated for bell-type distributions [23] and for the one-dimensional Jüttner (relativistic thermal) distribution

$$F(p) = \frac{ne^{-\rho\gamma}}{2\pi mcK_1(\rho)}, \tag{11}$$

where $\rho = mc^2/T$ is the inverse temperature in units of the rest energy of the electron ($\rho=1$ corresponds to $T\approx 5\times 10^9$ K), $K_n(\rho)$ is a modified Bessell function. The results are not particularly sensitive to the form of the distribution function, suggesting that useful analytic approximations might be found in terms of the mean Lorentz factor $\langle\gamma\rangle$. In the following we choose the Jüttner distribution (11), in which case one has $\langle\gamma\rangle \approx 1/\rho$ in the highly relativistic limit $\rho \ll 1$. The moments $\langle\gamma^n\rangle$ for relevant (positive and negative) integer n were written down in Ref. [6].

Relatively simple approximations to the RPDFs can be obtained when the distribution is an even function of β. One may write Eq. (4) in terms of integration over γ. Then the RPDFs in the plasma rest frame are given by

$$R(z) = \frac{\gamma_z^2 z}{2}\left\langle \frac{1}{\gamma-\gamma_z} + \frac{1}{\gamma+\gamma_z}\right\rangle, \tag{12}$$

$$S(z) = \frac{\gamma_z z}{2}\left\langle \frac{1}{\gamma-\gamma_z} - \frac{1}{\gamma+\gamma_z}\right\rangle, \tag{13}$$

where $\gamma_z = 1/(1-z^2)^{1/2}$ with $|z| \lesssim 1$. For $z=z_\pm$, one may write

$$\gamma_\pm^2 = \left[\frac{yz \pm (1+y^2-z^2)^{1/2}}{1-z^2}\right]^2. \tag{14}$$

One may express $W(z)$ in terms of $R(z)$ and its derivative, i.e.,

$$W(z) = -2zR(z) + (1-z^2)R'(z) - \frac{K_0(\rho)}{K_1(\rho)}, \tag{15}$$

where $\langle\gamma^{-1}\rangle = K_0(\rho)/K_1(\rho)$ and $R(z)$ is extended to $-\infty < z < \infty$.

A. Cyclotron resonance

There are four contributions to the dispersion associated with Eqs. (12) and (13): contributions associated with the resonances at $\gamma=\gamma_\pm$ and contributions associated with the resonances at $\gamma=-\gamma_\pm$. A physical interpretation of these four contributions follows by considering the solutions of the resonance condition $\omega(1-\beta\cos\theta) - s\Omega_e = 0$, where the refractive index is set to unity and with $s=+1$ for cyclotron absorption and $s=-1$ for anomalous Doppler emission [29]. Setting $\beta = \pm\cos\theta/|\cos\theta|$ the Doppler condition implies $\gamma = s\Omega_e(1\pm|\cos\theta|)/\omega\sin^2\theta$. Inspection of Eq. (14) for $z \to 1/\cos\theta$, $y \to \Omega_e/\omega\cos\theta$, one finds that for $\Omega_e \gg \omega\sin^2\theta$ the solutions of the resonance condition correspond to $\gamma = s\gamma_\pm$. Hence, the terms involving $1/(\gamma-\gamma_\pm)$ in Eqs. (12) and (13) correspond to cyclotron absorption, with the plus sign for a resonant particle traveling in the same direction as the wave $\beta \to \cos\theta/|\cos\theta|$ and the minus sign for a resonant particle traveling in the opposite direction to the wave $\beta \to -\cos\theta/|\cos\theta|$. Cyclotron absorption by particles with a given γ of waves with a given θ occurs at two different frequencies for forward and backward particles, with these frequencies in the ratio $(1+|\cos\theta|)/(1-|\cos\theta|)$.

Note that cyclotron absorption for both $\beta \to \pm\cos\theta/|\cos\theta|$ in the rest frame of the plasma can correspond to cyclotron resonance between outgoing particles and outgoing waves in the pulsar frame. The $\pm$ solutions then correspond to two absorption bands. The contribution to the dispersion corresponding to cyclotron absorption is most important when the relevant resonance occurs in the physical region, specifically for $\gamma_\pm \lesssim \langle\gamma\rangle$. For $\omega \ll \Omega_e/\langle\gamma\rangle$ the resonances occur in the tail of the distribution, and for $\omega \gtrsim \Omega_e/\langle\gamma\rangle$ the resonances occur in the nonrelativistic region,

where there are few particles. Cyclotron resonance is possible only for $\sin^2\theta \leqslant (\Omega_e/\omega)^2$ (for $\omega^2 \leqslant \Omega_e^2 + k_\parallel^2 c^2$ more generally).

The terms involving $1/(\gamma+\gamma_\pm)$ in Eqs. (12) and (13) correspond to anomalous cyclotron emission, which is outside the physical region when the refractive index is equal to unity. Although anomalous Doppler emission is forbidden, the associated contributions, for $\beta \to \pm\cos\theta/|\cos\theta|$, to the dispersion are nonzero, but generally small. The contribution of the anomalous Doppler resonance is retained in the following discussion.

B. RPDFs in terms of the exponential integral function

For the Jüttner distribution (11) in the relativistic limit $\rho \ll 1$, the relevant RPDFs are well approximated in terms of the exponential integral functions [27]

$$R(z) \approx -\frac{1}{2}\rho\gamma_z^2 z[e^{-\rho\gamma_z}\mathrm{Ei}(\rho\gamma_z) + e^{\rho\gamma_z}\mathrm{Ei}(-\rho\gamma_z)], \quad (16)$$

$$S(z) \approx -\frac{1}{2}\rho\gamma_z z[e^{-\rho\gamma_z}\mathrm{Ei}(\rho\gamma_z) - e^{\rho\gamma_z}\mathrm{Ei}(-\rho\gamma_z)], \quad (17)$$

$$W(z) \approx -\rho\gamma_z^2\left\{1 - \frac{1}{2}\rho\gamma_z z^2[e^{-\rho\gamma_z}\mathrm{Ei}(\rho\gamma_z) - e^{\rho\gamma_z}\mathrm{Ei}(-\rho\gamma_z)]\right\}, \quad (18)$$

$$W(z) \approx \rho\gamma_*^2\left\{1 - \frac{1}{2}i\rho\gamma_* z^2[e^{-i\rho\gamma_*}\mathrm{Ei}(\rho(i\gamma_*+1)) - e^{i\rho\gamma_*}\mathrm{Ei}(-\rho(i\gamma_*-1))]\right\}, \quad (19)$$

where the last expression is for $|z| \geqslant 1$ with $\gamma_* = i\gamma_z$ and $\mathrm{Ei}(x)$ is the exponential integral function. In deriving Eq. (19) we use a more general form of the exponential integral function, whose argument extends to include the whole upper complex plane (see the Appendix).

Two relevant approximation regimes are considered here: $\rho\gamma_z \ll 1$ and $\rho\gamma_z \gg 1$. In the former case one may make an expansion of $e^{\mp\rho\gamma_z}\mathrm{Ei}(\pm\rho\gamma_z)$ in $\rho\gamma_z \ll 1$. One obtains the following approximate expressions:

$$R(z) \approx -\rho\gamma_z^2 z[\ln(\rho\gamma_z) + C], \quad (20)$$

$$S(z) \approx (\rho\gamma_z)^2 z[\ln(\rho\gamma_z) + C - 1], \quad (21)$$

where $C \approx 0.577$ is Euler's constant. In the latter case $\rho\gamma_z \gg 1$, one has

$$R(z) \approx -\frac{1}{\rho}\left[1 + \frac{6}{(\rho\gamma_z)^2}\right], \quad (22)$$

$$S(z) \approx -\left[1 + \frac{2}{(\rho\gamma_z)^2}\right]. \quad (23)$$

From Eq. (15) or (19) with Eqs. (22) and (23), one obtains

$$W(z) \approx -\rho\gamma_z^2\{1 - \rho^2\gamma_z^2 z^2(\ln\rho\gamma_z + C)\} \quad (24)$$

for $|z| \ll (1-\rho^2)^{1/2}$ and

$$W(z) \approx \rho\gamma_*^2\{1 + \rho^2\gamma_*^2 z^2(\ln\rho + C)\} \quad (25)$$

for $|z| \gg (1-\rho^2)^{1/2}$. For $\rho\gamma_z \gg 1$, one has the expansion

$$W(z) \approx \frac{2}{\rho}\left[1 + \frac{12}{(\rho\gamma_z)^2}\right], \quad \rho\gamma_z \gg 1. \quad (26)$$

V. WAVE DISPERSION NEAR CYCLOTRON RESONANCE

The dispersion relation implied by Eq. (5) can be rewritten as

$$n_\pm^2 = 1 + t_+ \mp (t_-^2 + 4t_3^2)^{1/2}, \quad (27)$$

with $t_\pm = (c^2/2\omega^2)(t_1^1 \pm t_2^2)$, and $t_3 = i(c^2/2\omega^2)t_2^1$. The leading order expression in the weak anisotropy approximation corresponds to $n_\pm = 1$. The next order approximation is found by substituting $n_\pm = 1$ into the right-hand side of Eq. (27), and higher order approximations are obtained by iteration. In this section we consider only the first order approximation in which $t_\pm$ and t_3 are evaluated at $n_\pm = 1$. For $n_\pm = 1$ one has

$$z_\pm = \frac{(\omega^2/\Omega_e^2) \pm [\omega^2/\Omega_e^2 + (1 - \omega^2/\Omega_e^2)/\cos^2\theta]^{1/2}}{1 + (\omega/\Omega_e)^2\cos^2\theta}\cos\theta. \quad (28)$$

Plots of $\gamma_\pm = 1/(1-z_\pm^2)^{1/2}$ as a function of ω/Ω_e in the small angle approximation are shown in Fig. 1. Near the cyclotron resonance one has large $\gamma_+ = 1/(1-z_+^2)^{1/2} \gg 1$. Cyclotron resonance is possible only in the frequency range $\omega^2 \leqslant \Omega_e^2/(1 - n_\pm^2\cos^2\theta) \approx \Omega_e/\sin^2\theta$ and within this frequency range z_+ is positive for forward propagation ($\theta < \pi/2$), and is generally sensitive to the propagation angle. In contrast, z_- is not particularly sensitive to the propagation angle in the $\theta \ll 1$ limit (except for near $\omega \sim \Omega_e/\theta$) and changes sign at $\omega = \Omega_e$. One has $z_- \approx -1 + 2\omega^2/\Omega_e^2$ for $\omega \ll \Omega_e$ and $z_- \approx 1 - 2\Omega_e^2/\omega^2$ for $\omega \gg \Omega_e$.

Assuming $n_\pm = 1$, one obtains

$$t_\pm = -\frac{\omega_p^2}{2\omega^2}\left\{W(\csc\theta)\tan^2\theta + \frac{\omega^2}{\Omega_e^2 + \omega^2\cos^2\theta} \times\left[(1 \pm \cos^2\theta)\left\langle\frac{1}{\gamma}\right\rangle + \frac{1}{z_+ - z_-}\sum_{\alpha=\pm}\alpha \times[(\cos\theta - z_\alpha)^2 \pm (1 - z_\alpha\cos\theta)^2]R(z_\alpha)\right]\right\}, \quad (29)$$

$$t_3 = -\eta\frac{\omega_p^2}{2\omega^2}\frac{\Omega_e\omega}{\omega^2\cos^2\theta + \Omega_e^2}\frac{1}{z_+ - z_-} \times\sum_{\alpha=\pm}\alpha(\cos\theta - z_\alpha)S(z_\alpha), \quad (30)$$

where $z_\pm$ are given by the approximation (28).

A. Approximation at small propagation angles

In the small angle approximation ($\theta \ll 1$) one has $\gamma_z = 1/(1-z^2)^{1/2} \gg 1$ [see Fig. 1(a)]. Assuming $z_+ = 1$ and using

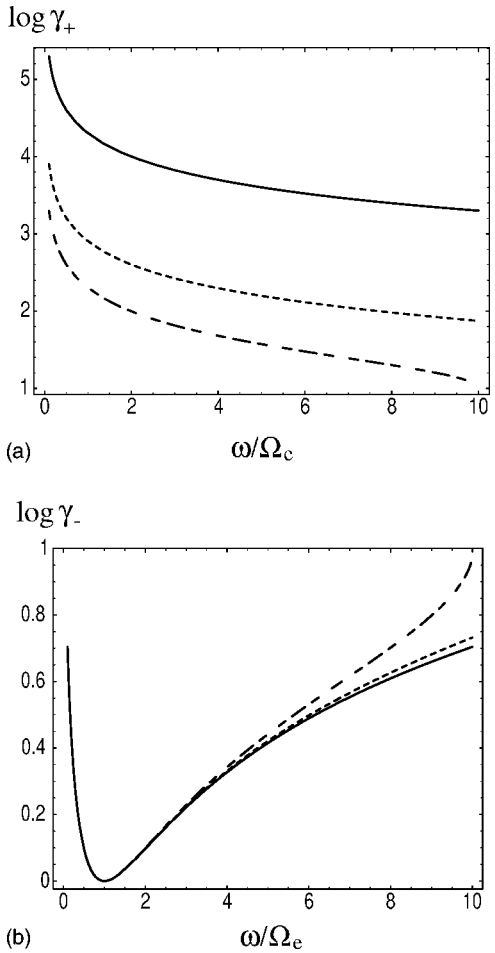

FIG. 1. Plots of $\gamma_{\pm}=1/(1-z_{\pm}^2)^{1/2}$ as a function of ω/Ω_e for small propagation angles $\theta \ll 1$. One assumes $n_{\pm}=1$ and $\theta=0.01$ (solid), $\theta=0.05$ (dotted), $\theta=0.1$ (dashed). Note that z_- is negative for $\omega/\Omega_e \leqslant 1$, to the left of the minimum in (b).

the expansions (20) and (21) for $R(z_-)$ and $S(z_-)$ one obtains

$$t_+ \approx -\frac{\omega_p^2}{\omega^2\rho}\left\{\theta^2+\frac{\omega^2\rho^2}{\omega^2+\Omega_e^2}\left[1+\frac{z_-}{1+z_-}\ln\left(\frac{\rho}{(1-z_-^2)^{1/2}}\right)\right]\right\}, \tag{31}$$

$$t_- \approx -\frac{\omega_p^2}{\omega^2}\frac{\theta^2}{\rho}, \tag{32}$$

$$t_3 \approx \eta\frac{\omega_p^2}{\omega^2+\Omega_e^2}\frac{\Omega_e}{2\omega}\frac{\rho^2 z_-}{(1-z_-^2)}\ln\left(\frac{\rho}{(1-z_-^2)^{1/2}}\right), \tag{33}$$

where $\langle 1/\gamma\rangle \approx \rho$, $W(\csc\theta)\approx 2/\rho$, and one keeps only the logarithmic terms in the expansions of $R(z_-)$ and $S(z_-)$. The corresponding approximate expression for the refractive index is

$$n_{\pm}^2 \approx 1-\frac{\omega_p^2}{\omega^2\rho}\left\{\theta^2+\frac{\omega^2\rho^2}{\omega^2+\Omega_e^2}\left[1+\frac{1}{2}\left(1-\frac{\Omega_e^2}{\omega^2}\right)\times\ln\left(\frac{\rho}{2}\frac{\omega^2+\Omega_e^2}{\omega\Omega_e}\right)\right]\pm\left[\theta^4+\frac{1}{16}\eta^2\rho^6\left(\frac{\omega}{\Omega_e}-\frac{\Omega_e}{\omega}\right)^2\times\ln^2\left(\frac{\rho}{2}\frac{\omega^2+\Omega_e^2}{\omega\Omega_e}\right)\right]^{1/2}\right\}, \tag{34}$$

where $z_-\approx(\omega^2-\Omega_e^2)/(\omega^2+\Omega_e^2)$ is used. The next order approximation to the refractive index can be obtained by substituting Eq. (34) for $n_{\pm}$ on the right-hand side of Eq. (27). The refractive indices (34) vary smoothly over the cyclotron resonance.

The polarization axial ratio can be written in the form

$$T_{\pm}\approx\frac{4}{\eta\rho^3}\frac{\omega\Omega_e}{\omega^2-\Omega_e^2}\left\{-\theta^2\pm\left[\theta^4+\frac{1}{16}\eta^2\rho^6\left(\frac{\omega}{\Omega_e}-\frac{\Omega_e}{\omega}\right)^2\times\ln^2\left(\frac{\rho}{2}\frac{\omega^2+\Omega_e^2}{\omega\Omega_e}\right)\right]^{1/2}\right\}\left[\ln\left(\frac{\rho}{2}\frac{\omega^2+\Omega_e^2}{\omega\Omega_e}\right)\right]^{-1}. \tag{35}$$

The approximate expressions (35) satisfy the orthogonality condition $T_+T_-=-1$. At $\omega\sim\Omega_e$ one has $T_-\to\pm\infty$ and $T_+\to 0$. In the small angle approximation, the dominant term in t_3 is $S(z_-)$, and the sign of $T_{\pm}$ is determined by the sign of z_-. Hence both polarization ellipses reduce to lines at $\omega=\Omega_e$ where they change their handednesses.

For a backward propagating wave, one has the same expressions for $n_{\pm}^2$ and $T_{\pm}$ as in Eqs. (34) and (35) except that the sign of $T_{\pm}$ is opposite to that for forward propagation. This can be shown by writing $\theta=\pi/2-\delta\theta$ with $\delta\theta\ll 1$ in Eq. (10). Since $W(z)$ is an even function of z and both $R(z)$ and $S(z)$ are odd functions of z, one can show that $t_{\pm}$ and t_3 have the same form as Eq. (33) except that t_3 has the opposite sign to that for forward propagation.

B. Perpendicular propagation

One may also derive an analytical approximation for dispersion for the case of perpendicular propagation by substituting $\theta=\pi/2-\delta\theta$ with $|\delta\theta|\ll 1$ in Eq. (30). One obtains

$$t_{\pm}\approx-\frac{\omega_p^2}{2\omega^2}\left\{\rho\delta\theta^2+\frac{\omega^2}{\Omega_e^2+\omega^2\delta\theta^2}\left[\rho\pm\frac{1\pm(1-\omega^2/\Omega_e^2)}{(1-\omega^2/\Omega_e^2)^{1/2}}\times R((1-\omega^2/\Omega_e^2)^{1/2})\right]\right\},$$

$$t_3\approx-\eta\frac{\omega_p^2}{2\omega^2}\frac{\Omega_e\omega}{\omega^2\delta\theta^2+\Omega_e^2}\frac{(1+\omega^2/\Omega_e^2)\delta\theta}{2(1-\omega^2/\Omega_e^2)^{1/2}}\times S((1-\omega^2/\Omega_e^2)^{1/2}), \tag{36}$$

where $z_{\pm}\approx\pm(1-\omega^2/\Omega_e^2)^{1/2}\delta\theta/|\delta\theta|+(\omega^2/\Omega_e^2)\delta\theta$ is used. Since $t_3=0$ for $\delta\theta=0$, both modes are linearly polarized at $\theta=\pi/2$. For $\omega\ll\Omega_e$ the approximation (36) can be further simplified to

$$t_+\approx\frac{\omega_p^2}{\Omega_e^2\rho}, \tag{37}$$

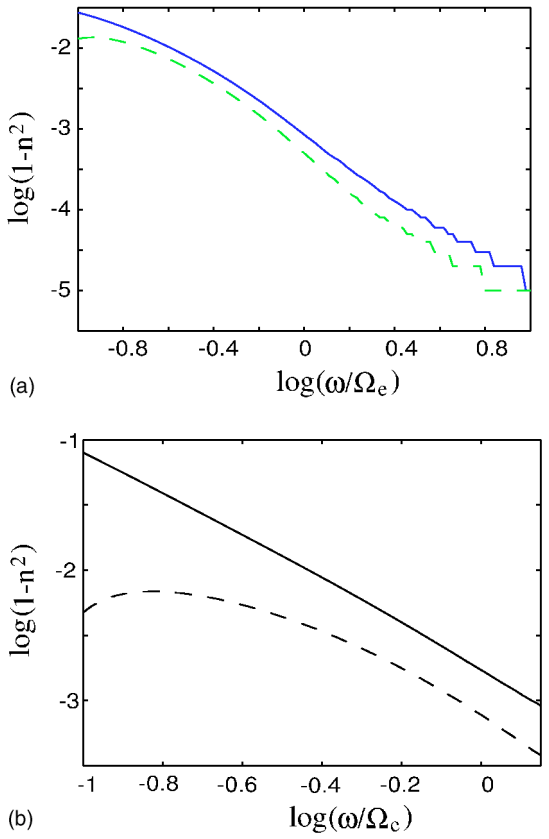

FIG. 2. Dispersion relation in the weak anisotropy approximation. The solid and dashed lines correspond to the + and − modes, respectively. The parameters chosen are $\theta=0.1$ (upper), $\theta=\pi/4$ (lower), $\rho=0.1$, $\omega_p/\Omega_e=0.1$.

$$t_- \approx -\frac{\omega_p^2}{2\omega^2}\left(\rho\delta\theta^2+\frac{\omega^4}{\Omega_e^4\rho}\right), \tag{38}$$

$$t_3 \approx \eta\frac{\omega_p^2}{2\omega\Omega_e}\left(\frac{\delta\theta}{2}\right). \tag{39}$$

From Eq. (27), the corresponding approximate form of the refractive indices can be written in terms of Eqs. (37)–(39).

C. Numerical calculation

It is straightforward to treat the dispersion in the weak anisotropy approximation by iteration of Eq. (27). Let $n_\pm^{(i)}$ be the ith order approximation to $n_\pm$ with $n_\pm^{(0)}=1$ the leading approximation. The RPDFs are evaluated by numerical integration and one can find $n_\pm^{(i-1)}$ and $n_\pm^{(i)}$ by iteration such that a prescribed accuracy is achieved. We choose $|n_\pm^{(i)}-n_\pm^{(i-1)}|<\epsilon$, with an accuracy $\epsilon=10^{-9}$. Figure 2 shows dispersion relations for two orthogonal modes derived from Eq. (27) using Eq. (10). The parameters chosen are $\rho=0.1$ and $\omega_p/\Omega_e=0.1$. As expected for a non-neutral plasma, the relevant modes are elliptically polarized. The refractive indices are very close to unity indicating that the weak anisotropy approximation is valid. The two modes are superluminal throughout the resonance region with their dispersion varying smoothly over the cyclotron resonance. The corresponding polarization ellipse is shown in Fig. 3. For $\theta\ll 1$, the sign change occurs at $\omega\sim\Omega_e$ and for much larger angles, it occurs at a frequency well below the cyclotron frequency, e.g., for $\theta=\pi/4$, the sign change occurs at $\omega\sim 0.6\Omega_e$.

To check the validity of the weak anisotropy approximation we need to compare the results with numerical results for the full dispersion equation in relevant cases. The full dispersion is obtained following the same precedure used in Ref. [24], i.e., by numerically finding roots of $\det(\Lambda^{ij})=0$, where $i,j=1,2,3$, and $\Lambda^i_j=-[k^ik_j+(t^H)^i_j]c^2/\omega^2-n^2g^i_j$, $(t^H)^i_j$ is the Hermitian part of the response tensor. For numerical efficiency we use the approximations (16)–(19) for the RPDFs. Examples of the calculations that include the cyclotron resonance are shown in Figs. 4 and 5. The dispersion curves derived in the weak anisotropy approximation agree well with the numerical solutions of the full dispersion equation. The polarization axial ratio near $\omega\sim\Omega_e$ is also consistent with the result from the full dispersion solution. In particular, the frequency at which the ellipses change their handedness is well approximated by the weak anisotropy limit. There is significant deviation at low frequencies due to the presence of the longitudinal component, in particular when ω is close to the plasma frequency.

VI. APPLICATION TO PULSAR RADIO EMISSION

The result on wave propagation through the cyclotron resonance region may be directly relevant for the interpretation of the observed polarization features of the pulsar radio emission. Observations of single pulses often reveal rapid change of circular polarization, i.e., in both its handedness and fraction in the total polarized radiation, across the pulse phase [14]. It is generally believed that the polarization features including such rapid variation in circular polarization are due to propagation effects. These features can be interpreted as the characteristics of the PLR, where the characteristic distance over which the two modes get out of phase is approximately equal to the characteristic distance over which the shape of the polarization ellipses of the two natural modes changes most rapidly. One strong possibility is that the PLR is located in proximity to the cyclotron resonance region where one expects the polarization ellipse to vary rapidly.

In the application to the interpretation of the rapid change in the handedness of circular polarization, one may consider a qualitative model in which the radio emission is assumed to be generated in the polar cap region well inside the light cylinder (the radial distance at which the rotation speed $=c$) at frequencies well below the cyclotron frequency. The radio emission eventually propagates through the cyclotron resonance region. Assume the radio emission propagates in one or superposition of the two natural modes. As shown in Fig. 3, the handedness of the two modes reverses and passes through 0 and ∞ at $\omega\sim\Omega_e$ in the plasma rest frame. Since the observed polarization should be characteristic of the PLR, which strongly depends on the plasma density, the handedness observed at one particular frequency depends on whether the PLR is located below or above the cyclotron

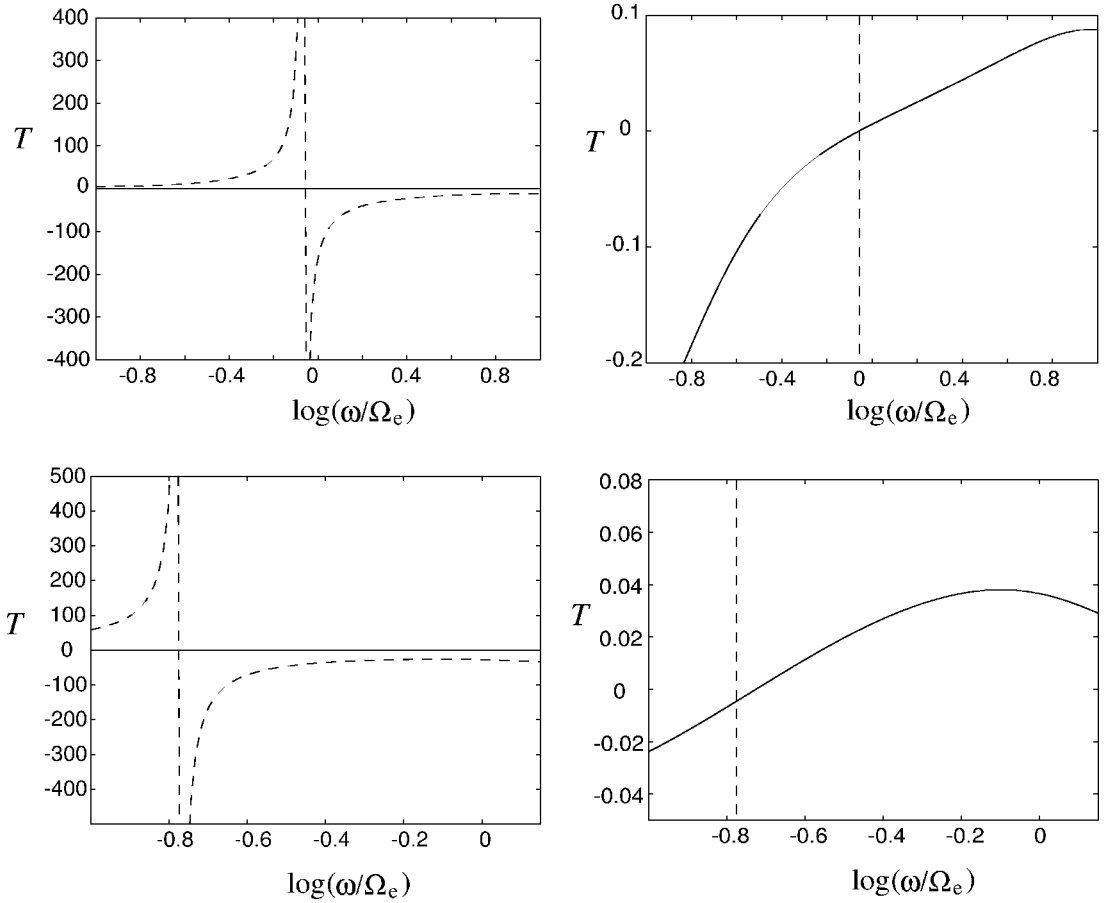

FIG. 3. Plots of $T_{\pm}$ as a function of ω/Ω_e. The solid and dashed curves correspond, respectively, to T_+ and T_-. The subfigures on the left are on a large acale and the soild lines, which vary only between ±1, appear almost along the axis. The vertical dashed line indicates the frequency at which the polarization is linear. The subfigures on the right show T_+ on a smaller scale. Upper: $\theta=0.1$; lower: $\theta=\pi/4$. In general, both modes are elliptically polarized and become linear at $\omega\sim\Omega_e$ for a small propagation angle and $\omega<\Omega_e$ for an intermediate propagation angle. Therefore both polarization ellipses change their sign in that region.

resonance layer. The pulsar plasma can be nonstationary as the result of a time-dependent pair cascade, as well as highly inhomogeneous in both along and transverse to the magnetic field lines. Therefore, one expects the actual location of the PLR to be randomly distributed across the cyclotron layer ($\omega\sim\Omega_e$ in the plasma rest frame). This may lead to random change in the handedness of circular polarization.

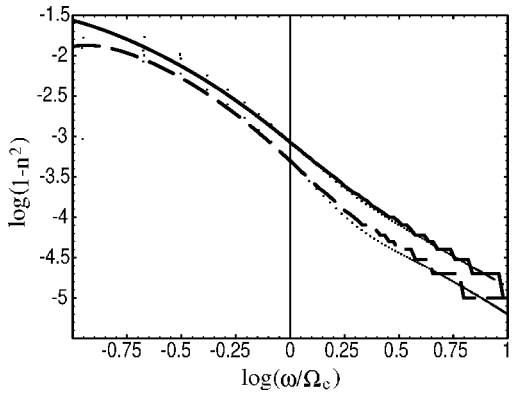

FIG. 4. The wave dispersion obtained from the full dispersion relation. The paramaters are the same as in Fig. 2(a). The solid dots represent the numerical solution of the full dispersion equation.

VII. CONCLUSIONS AND DISCUSSION

In this paper we discuss the effect of an intrinsically relativistic distribution of particle momenta on wave dispersion in the cyclotron resonance region, assuming that this is much higher than the plasma frequency. A highly relativistic spread in momenta smears out the familiar cyclotron resonance in a nonrelativistic plasma, such that the wave dispersion varies slowly across the cyclotron region, with no evidence of a resonance in dispersion curves. It is shown that the weak anisotropy approximation is then adequate for study of the wave properties in the cyclotron region. One major advantage is that the weak anisotropy approximation allows one to derive relatively simple analytical expressions for the wave dispersion and polarization axial ratios. Specificaly, approximate expressions for the cases of nearly forward, nearly backward, and nearly perpendicular propagation waves are derived in Sec. V.

A notable consequence of the relativistic effects is on the polarization ellipse, which changes its handedness as the cy-

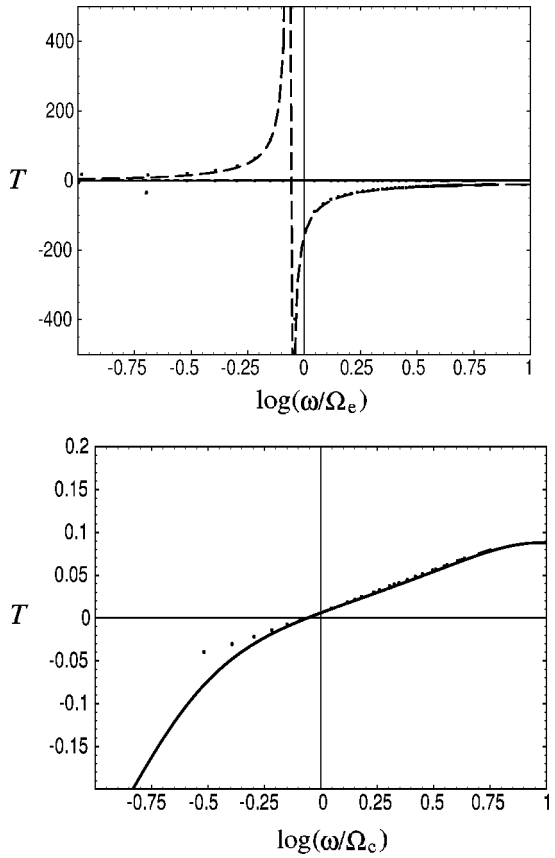

FIG. 5. Plots of $T_{\pm}$ as a function of ω/Ω_e as in Fig. 3 (upper). Upper: Comparison with the numerical solution of the full dispersion equation, represented by the solid dots. The vertical dashed line indicates the transition of the polarization ellipses. The plots of T_+ with the dots for the full solution and solid line for the weak anisotropic solution are very close to the horizontal axis. Lower: A zoom-in plot of T_+. The weak anisotropic solution is hardly distinguishable from the full dispersion solution at frequency $\omega \gg \omega_p$.

clotron region is crossed. Such a change occurs at the cyclotron resonance in a nonrelativistic plasma, and although the resonance itself is smeared out by relativistic effects, the change in handedness remains. Thus, as the cyclotron resonance is crossed (for example, as radiation escapes towards decreasing B), the main effect in the cyclotron region is the change in the shape of the polarization ellipse, and the change in its handedness (at the point where the natural modes are linearly polarized).

We propose to apply the results derived here to discuss circular polarization in pulsar radio emission. It is plausible that the polarization is characteristic of a PLR and that such region is located in the cyclotron region where the most rapid change in the shape of the polarization ellipse occurs and where the handedness reverses and the axial ratios for the two modes passes through 0 and ∞. Thus, it is plausible that the observed polarization is frozen in at this position and that change of its handedness is due to change of the location of the PLR relative to the cyclotron region as the result of variation of the plasma density. A further quantitative analysis of this location requires not only the results derived in this paper for the dispersion, but also specific model for the spatial variations of the pulsar plasma through which the waves propagate. We propose to explore this problem elsewhere.

ACKNOWLEDGMENT

We thank Andrew Willes for useful comments.

APPENDIX: EXPONENTIAL INTEGRAL FUNCTIONS

The relevant exponential integral functions are defined by [28]

$$\mathrm{Ei}(x) = -\mathcal{P}\int_{-x}^{\infty} dt \frac{e^{-t}}{t}, \tag{A1}$$

$$\mathrm{E}_n(x) = \int_1^{\infty} dt \frac{e^{-xt}}{t^n}, \quad x > 0, \tag{A2}$$

where $n=0,1,2,\ldots$, and $\mathcal{P}$ denotes the Cauchy principal value. In terms of these integral functions, one has [27]

$$\int_1^{\infty} \frac{d\gamma\, e^{-\rho\gamma}}{\gamma \pm \gamma_z} = -e^{\pm\rho\gamma_z}\mathrm{Ei}(\mp\rho(\gamma_z \pm 1)), \tag{A3}$$

$$\int_1^{\infty} \frac{dt\, e^{-\rho\gamma}}{\gamma^s} = E_s(\rho), \tag{A4}$$

where for convenience one extends $\mathrm{Ei}(x)$ to the whole upper complex plane $\arg(x) < \pi$ by identifying $\mathrm{Ei}(x) = -\mathrm{E}_1(-x)$. Equations (A3) and (A4) are used to write the RPDFs in terms of the exponential integral function $\mathrm{Ei}(x)$.

[1] J. K. Daugherty and A. K. Harding Astrophys. J. **253**, 337 (1982).
[2] P. N. Arendt Jr., and J. A. Eilek, Astrophys. J. **581**, 451 (2002).
[3] J. C. Weatherall, Astrophys. J. **428**, 261 (1994).
[4] J. A. Hibschman and J. Arons, Astrophys. J. **560**, 871 (2001).
[5] D. B. Melrose, ASP Conf. Ser. **202**, 721 (2000).
[6] D. B. Melrose and M. Gedalin, Astrophys. J. **521**, 351 (1999).
[7] R. D. Blandford and E. T. Scharlemann, Mon. Not. R. Astron. Soc. **174**, 59 (1976).
[8] A. B. Mikhailovskii, O. G. Onishechenko, G. I. Suramlishvili, and S. Sharapov, Sov. Astron. Lett. **8**, 369 (1982).
[9] Q. Luo and D. B. Melrose, Mon. Not. R. Astron. Soc. **325**, 187 (2001).
[10] D. Fussell, Q. Luo, and D. B. Melrose, Mon. Not. R. Astron. Soc. **343**, 1248 (2002).

[11] M. M. McKinnon and D. R. Stinebring, Astrophys. J. **502**, 883 (1998).
[12] M. M. McKinnon and D. R. Stinebring, Astrophys. J. **529**, 435 (2000).
[13] J. L. Han, R. N. Manchester, R. X. Xu, and G. J. Qiao, Mon. Not. R. Astron. Soc. **300**, 373 (1998).
[14] A. Karastergiou, S. Johnston, and M. Kramer, Astron. Astrophys. **404**, 325 (2003).
[15] D. B. Melrose, Aust. J. Phys. **32**, 61 (1979).
[16] J. Barnard and J. Arons, Astrophys. J. **302**, 138 (1986).
[17] D. B. Melrose and Q. Luo, Mon. Not. R. Astron. Soc. (to be published).
[18] J. Arons and J. Barnard, Astrophys. J. **302**, 120 (1986).
[19] D. G. Lominadze, G. Z. Machabeli, G. I. Melikidze, and A. D. Pataraya, Sov. J. Plasma Phys. **12**, 712 (1986).
[20] M. Gedalin, D. B. Melrose, and E. Gruman, Phys. Rev. E **57**, 3399 (1998).
[21] D. B. Melrose, M. Gedalin, M. Kennett, and C. S. Fletcher, J. Plasma Phys. **62**, 233 (1999).
[22] E. Asseo and A. Riazuelo, Mon. Not. R. Astron. Soc. **318**, 983 (2000).
[23] M. P. Kennett, D. B. Melrose, and Q. Luo, J. Plasma Phys. **64**, 333 (2000).
[24] Q. Luo, D. B. Melrose, and D. Fussell, Phys. Rev. E **66**, 026405 (2002).
[25] V. N. Sazonov and V. N. Tsytovich, Radiophys. Quantum Electron. **11**, 731 (1968).
[26] D. B. Melrose, *Plasma Astrophysics* (Gordon and Breach, New York, 1980), Vol. 1.
[27] Q. Luo and D. B. Melrose, J. Plasma Phys. (to be published).
[28] M. Abramowitz and I. Stegun, *Handbook of Mathematical Functions* (Dover, New York, 1970), p. 228.
[29] A. Z. Kazebegi, G. Z. Machabeli, and G. I. Melikidze, Mon. Not. R. Astron. Soc. **253**, 377 (1991).